Preparation and Characterization of Nanocellulose/SA sponge for Hemostasis

Feng Cheng[1], Xinjing We[1], Tingsheng Yan[1] and Jinmei He[1*]

[1]MIIT Key Laboratory of Critical Materials Technology for New Energy Conversion and Storage, School of Chemistry and Chemical Engineering, Harbin Institute of Technology, Harbin 150001, People's Republic of China.

E-mail: hejinmei@ hit. edu. cn

Keywords: cellulose nanocrystals, oxidation, alginate, sponge, hemostatic

Introduction

Excessive hemorrhage is the main cause of pre-hospital trauma death during in both military and civilian trauma, and effective hemostatic materials can quickly prevent bleeding to reduce the mortality.[1, 2] Alginate (SA) dressings which have excellent hemostasis efficiency, are able to absorb large volumes of wound exudate while providing a physiologically moist microenvironment for wound healing, and can be easily removed from the wound site.[3, 4] However, due to their poor chemical stability and mechanical strength, and their uncontrollable structure degradation would conduce to the limited application of neat alginate.[5, 6] Cellulose is the most abundant renewable biopolymer composed of β-1-4-linked D-anhydroglucose units and is almost inexhaustible raw material, which has been used in a wide variety of applications.[7, 8] Cellulose nanocrystal (CN) has attracted a great deal of interests during the last decade in the nanocomposites field, owing to its impressive intrinsic properties including nanoscale features, high specific surface area, unique morphology, low density, mechanical strength, renewability and biodegradability.[9-12] Furthermore, the amount of active hydroxyl groups on the CN surface is suitable for chemical modification, such as oxidation and polymer grafting.[13] For instance, recent study reported that the regulation of blood metabolic variables by the presence of 2, 2, 6, 6-tetramethylpiperidine-1-oxyl (TEMPO)-oxidized cellulose nanofibers, which showed the promising hemocompatibility and unique biological activities.[14] TEMPO-mediated oxidized bacterial cellulose-sodium alginate composites have been prepared as a biomedical material to cell encapsulation, which showed TEMPO-mediated oxidized bacterial cellulose could improve the mechanical and chemical stability of the composites and would be a potential candidate for many biomedical applications.[15] This work aimed to design an effective hemostatic material for the wound healing and a possible hemostatic mechanism for TOCN (TEMPO-mediated oxidized cellulose nanocrystals)/SA composites is discussed.

Materials and Methods

Microcrystalline cellulose (99 %) was purchased from Shanghai Luan Biological Technology Co., Ltd (China). Sodium alginate was purchased from Sinopharm Chemical Reagent Co., Ltd (China). Sodium hypochlorite (NaClO) solution was purchased from Shuang Shuang Chemical Co., Ltd (Yantai, China). TEMPO

($C_9H_{18}ON$, 98%), sodium bromide (NaBr) and calcium chloride ($CaCl_2$) were purchased from Sinopharm Chemical Reagent Co., Ltd (China). All of the reagents were of analytical grade and used without further purification. Healthy rabbits and human blood were supplied by animal experiment center of the second affiliated hospital of Harbin medical university (Harbin, Heilongjiang Province, China). The protocol was approved by the ethics committee of the Harbin Medical University. All animals were handled according to the Chinese National Institutes of Health Guidelines for the Care and Use of Laboratory Animals.

Preparation of TOCN/SA Composite Sponge.

The method for the preparation of cellulose nanocrystal (CN) is well-documented in the literature. [16-19]Briefly, Acid hydrolysis was prepared at 35℃with 64 wt % H_2SO_4 (250mL) for 2h under the condition of continuous mechanical stirring and then MCC powder (10 g) was slowly added to suspension. The hydrolysis was terminated by adding a large amount of distilled water (more than 10 times volume of the H_2SO_4 solution which has been used). The system was still placed overnight at 4℃ and then the supernatant was discarded. After that, the system was centrifuged (10000 rpm) for 10 min each step (washed repeated over three times). Dialyzed with the distilled water for about 3-5 days, until was reached a neutral pH environment. After dialysis, the CN dispersion was used by ultrasonic treatment, and finally, the CN power was prepared by freeze-drying. TEMPO-mediated oxidation of CN (TOCN) was followed by the method described in the literatures.[19-22] Briefly, about 0.5 g CN was suspended in 50 mL distilled water and then ultrasonic dispersion treatment for 15 min. TEMPO (0.05 g, 0.32 mmol) and NaBr (0.5 g, 4.86 mmol) were dissolved in another 50 mL distilled water, which were added dropwise slowly to the CN dispersion. A certain quantity of 12 wt% NaClO (15mL, 46.5 M) solution was added slowly to the mixture to start the oxidizing reaction. When stirring the mixture for 3h, the pH of the mixture was remained at 10.8 by adding 0.5 M NaOH. TOCN was introduced in a certain amount of alginate solution for the preparation of cross-linked sponge. The detailed procedure was illustrated in Fig.1. The TOCN/SA composite suspension was casted in Petri dish plates, a portion of them freeze-dried. Cross-linked TOCN/SA composite sponges were prepared by $CaCl_2/H_2O/C_2H_5OH$ solution for 1h. And then washed with distilled water to remove residual Ca^{2+} ions and freeze-dried again to obtain the cross-linked sponges before.

Characterization

Scanning electron microscopy (SEM) analysis measurements were carried out by Quanta 200 FEG scanning electron microscope (FEI, Hong Kong) equipped with an energy dispersive spectroscopy detector. The morphologies of NC and TOCN were examined by transmission electron microscopy (TEM) (JEM-F 200, Japan) at an accelerating voltage of 80kV.

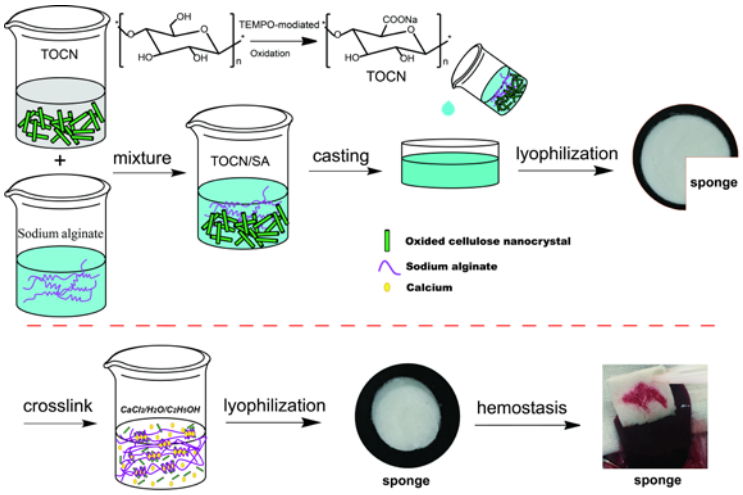

Fig.1 Scheme of preparation and application for TOCN/SA composite sponge.

Blood Cells and Platelet Adhesion

The blood cells and platelet adhesion were conducted as the reported literatures. 34-35 In brief, for whole blood cell and platelet adhesion determine, the TOCN/SA composite sponge was cut into 1×1 cm^2 and immersed into PBS (pH=7.2-7.4) for 1h at 37℃. Whereafter, the whole blood was added dropwise onto the sample and then incubated for 5min at 37℃. Platelet rich plasma (PRP) was separated from the whole blood by centrifugation of blood at 800 rpm for 10 min. Then, the PRP was added dropwise onto the sample and incubated for 1h at 37℃. All samples were then washed with PBS solution three times to remove the physical adhered blood cells and platelets, then fixed by using 2.5 % glutaraldehyde for another 2h. After that, blood cells and platelets were dehydrated with 50 %, 60 %, 70 %, 80 %, 90 %, and 100 % ethanol solution, with the interval for 10 min. Finally the samples were dried and SEM images were taken.

Hemostatic evaluation

Rabbit liver trauma model

The hemostatic behavior of the TOCN/SA composite sponges was estimated by covering them on the abraded liver of the male New Zealand White rabbits (which is 4 months old and around 3.5 kg). The composite sponges were cut into pieces of required size (2.0 cm×2.0 cm) and sterilized by the ultraviolet radiation for testing the hemostatic efficiency. Before undergoing an abdominal incision, the rabbits were fixed on the surgical cork board and then the ear marginal veins were injected with 3% pentobarbital sodium aqueous solution (30 mg/kg) to anaesthetize. The composite samples were applied to the liver wound immediately when the liver was pricked with a needle (the diameter is 2 mm, and the pricked depth is 3 mm), respectively. The hemostatic evaluation was detected every 30 s, then the hemostatic time and blood loss was recorded.

Rabbit ear artery model

After the anesthesia of ear marginal veins injected pentobarbital sodium solution, the auricular artery of the rabbit, in the middle of rabbit ear, was prepared and sterilized, and the blood vessels were torn by the scalpel blade. Then the composite samples were covered on the wound, then the hemostatic time and blood loss was recorded immediately.

Results

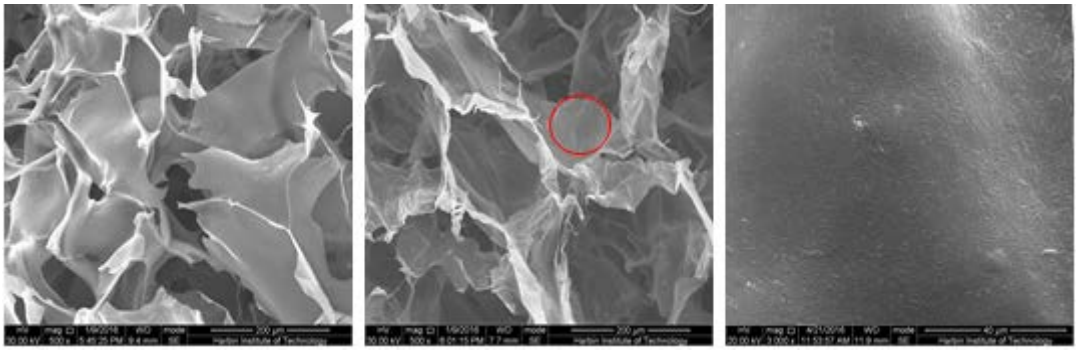

(a) (b) (c)

Fig.2 SEM images of the cross-section morphology of TOCN/SA composite sponge, uncross-linked sample (a), cross-linked sample (b) 500×, and cross-linked sample (c) 3000×.

Fig. 3 EDS spectrum of Ca^{2+} crosslinking for TOCN/SA composite sponge.

The SEM micrographs of the composite sponges were shown in Fig.2. When cellulose nanocrystals (TOCN) were introduced into SA, the rod-like shape nanocrystals appeared in the hole-wall of sponge (Fig.2b). In addition, there was no apparent self-aggregation or microphase separation in the sponge. The introduction of TOCN, build the more regular internal three-dimensional network of cross-linked TOCN/SA sponge than uncross-linked one. In addition, there was no obvious self-aggregation or microphase separation in the sponge. The results of EDS mapping showed that the Ca^{2+} was homogeneously distributed on both the superficial and cross-sectional surfaces of composite sponge (Fig. 3).

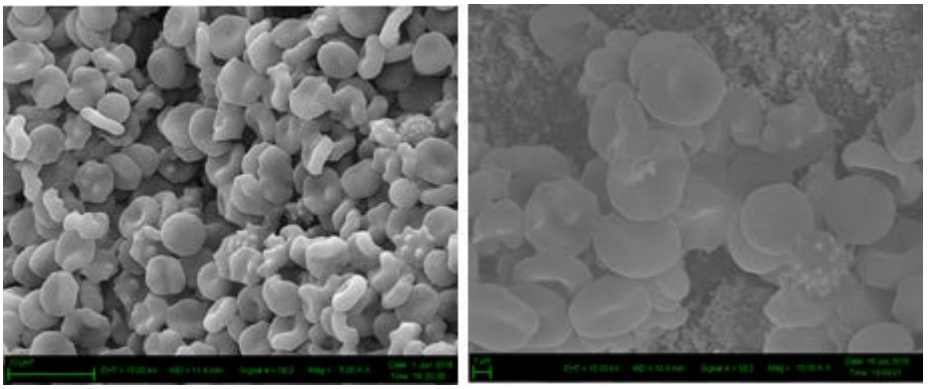

(a)

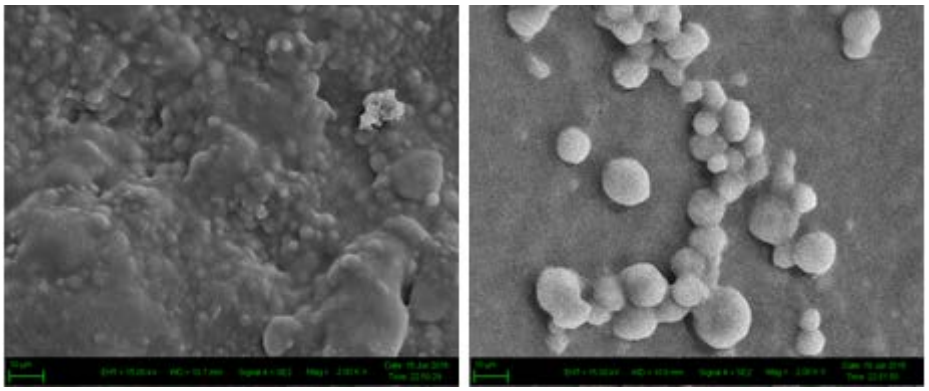

(b)

Fig. 4 SEM images of hemocyte and platelet adhesion. TOCN/SA composite sponge hemocyte adhesion (a), TOCN/SA composite sponge platelet adhesion (b), respectively.

In order to further reveal the hemostatic mechanism, the surface adhesion and morphologies of blood cells and platelets on the composite samples were observed by SEM. A large amount of erythrocytes gathered on the TOCN/SA composites surface and kept their distinctive biconcave disks, none of them exhibited deformation or aggregation (appeared in Fig.4 a). Moreover, there were no spiny pseudopodia for erythrocytes adsorbed on the materials surface. As shown in Fig. 8b, the amount of platelets adsorbed on the composites material surface and most of them were activated. In addition, significantly larger platelet aggregates and more platelets altered their shape from irregular distinctive disks to circular deformation on TOCN/SA composite sponge.

Evaluation of hemostatic properties of neat SA and TOCN/SA composite materials was exhibited by the amount of bleeding and hemostatic time both in rabbit liver injury model and ear artery injury model from Fig.5 and Table.1. In rabbit liver injury model, the amount of bleeding of the other groups were all significantly different from the gauze within a value of 1.735 ± 0.055g, and the amount of bleeding of TOCN-30/SA composite sponge (0.539±0.069g) were significantly lower than other materials (presented in Fig.5 b). There was no significantly difference between the bleeding amounts of TOCN-10/SA sponge (0.815±0.079g) and TOCN-50/SA sponge (0.789±0.056g). In addition, the hemostatic time of TOCN-30/SA composite sponge (76±8.13s) was the slowest one compared to other groups (Table.1). In rabbit

ear injury model, it was clearly showed in Fig.5 b. The amount of bleeding of all sponges groups were significantly lower than that of gauze (1.012±0.068g), and the average value of TOCN-30/SA composite sponge was the lowest one with the blood loss of 0.404±0.058g (Fig.5b). There was no significant difference between TOCN-10/SA composite sponge (0.503±0.058g) and TOCN-50/SA composite sponge (0.498± 0.065g). Moreover, when it came to the hemostatic speed of all materials, the average hemostatic speed of TOCN-30/SA composite sponge (70 ± 5.93s) was the shortest one (Table 1).

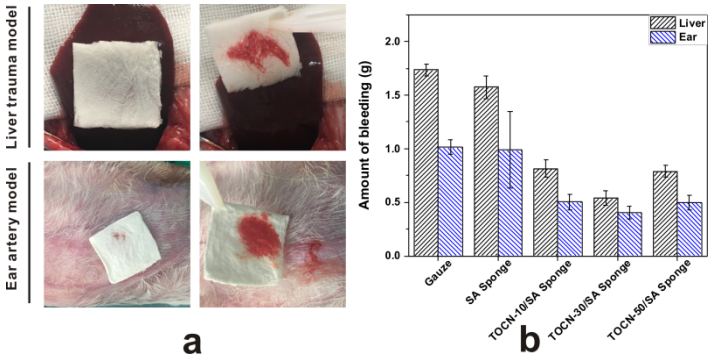

Fig. 5 The hemostatic effect of neat SA, TOCN/SA composite sponges on the different trauma of rabbit the liver and the ear artery (a). The amount of bleeding of neat SA and TOCN/SA composite sponges (b).

Discussion

Highly porous and interconnected pore structures are needed for alginate-based sponges to ensure water absorption and mechanical strength, especially as biomedical materials, such as tissue engineering scaffolds. Since the three-dimensional network structures were useful to nutrients metabolism metabolic wastes and beneficial to the growth and transport of cells, the vessels and tissues could grow successfully with materials implanted. Thus, the TOCN/SA composite sponge might accelerate the tissues healing within a shorter time biodegradation in vivo. The results of blood Cells and platelet adhesion indicated that the TOCN/ SA composite sponge would not affect physiological action of the blood cells. Incubation with platelet-rich plasma (PRP) was further to demonstrate the platelets adhesion on the TOCN/SA composites surface, which may attributed to the platelets were attracted and activated by the carboxyl groups. According to the these results, it might indicated that the porous structure and good swelling degree of the sponge were helpful to improve the adsorption ability for platelets and erythrocytes to achieve rapid hemostatic effect.The above mentioned results indicated that the TOCN-30/SA sponge has the potential to significant improve the hemostatic efficiency. The hemostatic effect of TOCN-30/SA composite sponge has excellent hemostatic properties including the blood loss and the hemostatic time (Fig.5b, Table.1). Firstly, TOCN-30/SA composite sponge had porous structure, which made to fast absorb the blood on the material surface with large capacity, and made more conducive to promoting the aggregation of platelets and inducing erythrocytes to accelerate blood clotting.[23] Secondly, the TOCN-30/SA composite sponge with hydrophilic carboxyl groups could combine Fe^{3+} in blood fluid to form the brown gel

and stimulate erythrocytes and platelets (GPIIb/IIIa) on the blood absorption process and also provide rapid hemostatic effect. Furthermore, TOCN/SA composite materials crosslinking with Ca^{2+}, which would activate blood coagulation by stimulating platelets and the clotting factors VII, IX and X in the blood clotting process.[24]In this study, when using TOCN/SA composite materials on the surface of wound, the materials containing Ca^{2+}, with excellent physical properties would absorb water from the blood, and aggregate the clotting factors to achieve hemostasis. It means that a rapidly coagulation rate would reduce the amount of bleeding and clots formation.

Table 1 The mean hemostatic time of SA and different TOCN/SA composites in two rabbit injury models

	Average hemostatic time (s)	
	Liver injury	Ear artery injury
Gauze	179 ± 8.99	130 ± 5.89
SA Sponge	186 ± 12.05	123 ± 13.38
TOCN-10/SA Sponge	92 ± 7.59	85 ± 10.37
TOCN-30/SA Sponge	76 ± 8.13	70 ± 5.93
TOCN-50/SA Sponge	80 ± 11.38	69 ± 10.08

Conclusion

2,2,6,6-Tetramethylpiperidine-1-oxyl (TEMPO)-mediated oxidized cellulose nano-crystals/alginate composite sponges were successfully prepared and simultaneously performed traditional Ca^{2+} cross-linked. Moreover, the TOCN-30/SA composite sponge had higher porosity and was helpful to absorb large abundant of wound exudate and improved the adsorption ability for platelets and erythrocytes to achieve rapid hemostatic effect. As a result, the hemostatic efficiency of the TOCN-30/SA composite sponge is the shortest one (about 70s) with the least blood loss in rabbit ear artery and liver trauma models, respectively. The hemostatic mechanism of TOCN/SA composite is the combination of physical adsorption and physiological hemostasis. Therefore, further study is essential for investigating the materials hemostatic mechanism and improving materials hemostatic efficiency used in the field of wound healing.

Acknowledgments

This work was financially supported by State Key Laboratory for Modification of Chemical Fibers and Polymer Materials, Donghua University (No. LK1510).

References

1. D. S. Kauvar, R. Lefering and C. E. Wade, *Journal of Trauma-Injury Infection and Critical Care*, 2006, **60**, S3-S9.
2. H. B. Alam, D. Burris, J. A. DaCorta and P. Rhee, *Military Medicine*, 2005, **170**, 63-69.
3. G. M. Jon A. Rowley, David J. Mooney, *Biomaterials*, 1999, **20**, 9.
4. K. G. H. A. Thomas, K. Moore, *Biomaterials*, 2000, **21**, 6.
5. S. Kalyani, B. Smitha, S. Sridhar and A. Krishnaiah, *Desalination*, 2008, **229**, 68-81.

6. G. Kaklamani, D. Cheneler, L. M. Grover, M. J. Adams and J. Bowen, *Journal of the mechanical behavior of biomedical materials*, 2014, **36**, 135-142.
7. N. Kanjanamosit, C. Muangnapoh and M. Phisalaphong, *Journal of Applied Polymer Science*, 2010, **115**, 1581-1588.
8. F. Cheng, J. He, T. Yan, C. Liu, X. Wei, J. Li and Y. Huang, *RSC Adv.*, 2016, **6**, 94429-94436.
9. R. J. Moon, A. Martini, J. Nairn, J. Simonsen and J. Youngblood, *Chemical Society reviews*, 2011, **40**, 3941-3994.
10. F. A. My Ahmed Said Azizi Samir, Alain Dufresne, *Biomacromolecules*, 2005, **6**, 15.
11. A. Dufresne, *Canadian Journal of Chemistry*, 2008, **86**, 484-494.
12. K. Ben Azouz, E. C. Ramires, W. Van den Fonteyne, N. El Kissi and A. Dufresne, *ACS Macro Letters*, 2012, **1**, 236-240.
13. N. Lin, J. Huang, P. R. Chang, J. Feng and J. Yu, *Carbohydrate Polymers*, 2011, **83**, 1834-1842.
14. N. Lin and A. Dufresne, *European Polymer Journal*, 2014, **59**, 302-325.
15. M. Park, D. Lee and J. Hyun, *Carbohydr Polym*, 2015, **116**, 223-228.
16. A. R. Lokanathan, K. M. Uddin, O. J. Rojas and J. Laine, *Biomacromolecules*, 2014, **15**, 373-379.
17. J. Song, G. Fu, Q. Cheng and Y. Jin, *Industrial & Engineering Chemistry Research*, 2014, **53**, 708-714.
18. E. Jin, J. Guo, F. Yang, Y. Zhu, J. Song, Y. Jin and O. J. Rojas, *Carbohydr Polym*, 2016, **143**, 327-335.
19. N. Lin, C. Bruzzese and A. Dufresne, *ACS Applied Materials & Interfaces*, 2012, **4**, 4948-4959.
20. F. Jiang and Y.-L. Hsieh, *ACS Sustainable Chemistry & Engineering*, 2016, **4**, 1041-1049.
21. F. Jiang and Y.-L. Hsieh, *J. Mater. Chem. A*, 2014, **2**, 350-359.
22. H. Koga, T. Saito, T. Kitaoka, M. Nogi, K. Suganuma and A. Isogai, *Biomacromolecules*, 2013, **14**, 1160-1165.
23. G. Lan, B. Lu, T. Wang, L. Wang, J. Chen, K. Yu, J. Liu, F. Dai and D. Wu, *Colloids and surfaces. B, Biointerfaces*, 2015, **136**, 1026-1034.
24. Q. Xia, Z. Liu, C. Wang, Z. Zhang, S. Xu and C. C. Han, *Biomacromolecules*, 2015, **16**, 3083-3092.